Desalination and Water Treatment
www.deswater.com
doi: 10.5004/dwt.2021.26637

212 (2021) 61–70
February

The facile synthesis of poly(acrylate/acrylamide) titanium dioxide nanocomposite for groundwater ammonia removal

Ali M. El Shafey, M.K. Abdel-Latif, H.M. Abd El-Salam*

Department of Chemistry, Faculty of Science, Polymer Research Laboratory, Beni-Suef University, 62514 Beni-Suef City, Egypt, emails: hanafya@yahoo.com/hanafy011246@science.bsu.edu.eg (H.M. Abd El-Salam), mly390861@gmail.com (A.M. El Shafey), m_kkhedr@yahoo.com (M.K. Abdel-Latif)

Received 14 April 2020; Accepted 2 October 2020

ABSTRACT

Recent researches are moving to the removal of the chemical contaminants from groundwater. The present work is to remove ammonia from groundwater based on acrylate/acrylamide hydrogel. This hydrogel was synthesized by the redox free radical addition polymerization technique. A nanocomposite of acrylate/acrylamide hydrogel with TiO_2 was fabricated. The synthesized hydrogel and composite were characterized by scanning electron microscopy, transmission electron microscopy, X-ray diffraction, and Fourier-transform infrared spectroscopy analysis. The influence of contact time, adsorbent dose, and temperature on the efficiency of the fabricated polymeric materials on the removal of ammonia from groundwater were investigated. The sorption data were analyzed and fitted to linearized adsorption isotherm of the Langmuir, Freundlich, and Temkin equations. The efficacy was equal to 100% through 50 min. The obtained data show both chemical and physical adsorption of ammonia.

Keywords: Acrylate/acrylamide hydrogel; Poly(acrylate/acrylamide) nanocomposite; Groundwater; Ammonia removal efficiency; Kinetic isotherms

1. Introduction

Water has an essential role in the living of all organisms. Many of the world's population do not have access to the drinking water of acceptable standards [1]. About 30% of the used water in the world is groundwater so, it is important another source of drinking where water naturally pure. The acceptable ammonia concentration in groundwater is ≤0.2 mg L^{-1} [2]. Ammonia is present in groundwater as ammonia nitrogen pollutants [3]. The uncontrollable use of fertilizers led to an increase in ammonia in surface and subsurface potable water [4]. The main sources of ammonia present in groundwater are; organic waste disposal or leaking sewage systems [5], chemical fertilizers [6], and environment originate from metabolic, agricultural, and industrial processes, in addition to disinfection with chloramines [7]. The problems of ammonia present in groundwater are; reduced water quality [8], accelerating the corrosion of the present construction materials [9], depletion of the dissolved oxygen in the water, presence of some algae toxin, phytoplankton blooms, and loss of livestock [10]. The impact of ammonia in water systems reflects on eutrophication of surface water and toxicity for fish [11]. Toxic levels of nitrite increase by increasing ammonia levels in drinking water [12]. So, the removal of ammonia from groundwater becomes the target of many researchers which can be achieved by different methods such as, nitrification/de-nitrification, ion exchange, air stripping, and adsorption [13]. Many researchers report the removal of ammonia and other undesirable metal ions such as lead, manganese copper, zinc, and iron by simple and low-cost methods [14–26]. Adsorption of ammonia on the surface of active inorganic, organic, polymeric materials and their composites are significant methods for the removal of ammonia

* Corresponding author.

from groundwater. Various materials were used for adsorption of ammonia such as bentonite, activated carbon, activated alumina, and zeolite [8]. Other materials were used for this target such as fly ash, zeolite, sepiolite, limestone, charcoal, bamboo charcoal, activated carbon, over burnet brick, activated clinoptilolite, and synthetic zeolite-A [27–35]. In the present work, cheap and easily prepared poly(acrylate/acrylamide) hydrogels and its composite are used as an adsorbent for the removal of ammonia present in groundwater. Synthesis of poly(acrylate/acrylamide) hydrogel was achieved by addition polymerization in presence of N,N′-methylenebisacrylamide as cross-linker and potassium persulfate (KPS) as initiator. The influence of contact time, adsorbent dose, and temperature on the sensitivity of the removal process were investigated. The synthesized polymeric samples were characterized by transmission electron microscopy (TEM), X-ray diffraction (XRD), and Fourier-transform infrared spectroscopy (FTIR) analysis respectively. The sorption data were analyzed and fitted to linearized adsorption isotherm of the Langmuir, Freundlich, and Temkin equations respectively. This hydrogel has been found to be an efficient adsorbent for the removal of ammonia from groundwater (>98% removal) and could be regenerated efficiently (100%).

2. Experimental section

2.1. Materials

Acrylic acid 99%, N,N′-methylenebisacrylamide 99% (cross-linker), KPS, and dimethylformamide 99.9% were products of Sigma-Aldrich (Germany). Acrylamide 98% was procured from the Oxford Company (India), hydrochloric acid 33%, sodium hydroxide pellets 98% were products of Prolabo Chemical Company (England). Acetone 99.5% and methanol 99.5% were provided by El-Nasr Pharmaceutical Chemical Company (Egypt). All the above chemicals are used as procured. titanium dioxide was provided from Loba Chemie, India. The water used in all experiments is distilled water.

2.2. Synthesis of poly(acrylate/acrylamide) hydrogel

Acrylic acid (3.70 mL = 0.05 mol) was neutralized with 2 g sodium hydroxide (0.05 mol in total volume 20 mL). Acrylamide (3.55 g = 0.05 mol) dissolved in 20 mL distilled water was added to the acrylate solution, 0.1 g of N,N′-methylenebisacrylamide as cross-linker was added to the above monomers solution. KPS (0.1 g) as initiator was used for this polymerization process under the nitrogen atmosphere at 60°C for 3 h. The quantity of both cross-linker and KPS was chosen based on the yield of the hydrogel. The formed hydrogel was separated, washed, and dried under vacuum at 70°C till constant.

2.3. Synthesis of TiO_2 nanoribbons

The alkaline hydrothermal method was applied for the synthesis of TiO_2 nanoribbons (TNRs). 4 g of TiO_2 powder was dissolved in 400 mL of 10 M NaOH and stirred for 30 min. The obtained solution was poured into a 1 L autoclave. Then, the autoclave was introduced to an oven for 24 h at 170°C. After that, the product was separated and washed with 0.1 M HCl and distilled water.

Finally, the obtained white powder was dried at 80°C for 4 h and calcined at 450°C for 2 h [36].

2.4. Fabrication of poly(acrylate/acrylamide) hydrogel/ TiO_2 composite

TNRs (0.1 g dissolved in 20 mL distilled water) was added during the synthesis of poly(acrylate/acrylamide) hydrogel. The obtained composite after 3 h was separated, washed, and finally dried till constant weight at 70°C. Also, the quantity of TNRs was chosen based on the yield of the composite.

2.5. Instrumental techniques

The infrared measurements were carried out using Shimadzu FTIR Vertex 70 Bruker Optics (Japan) technique to identify the functional groups for both synthesized hydrogel and their composite. FTIR spectra of the samples were recorded from 400 to 4,000 cm^{-1} using KBr pellets at room temperature.

2.6. Morphological studies

The XRD patterns of synthesized hydrogel and its composite were characterized using PANalytical Empyrean X-ray diffractometer 202964. The scan range was (5°–140°). The electron microscopic pictures were taken using JSM-6510LA scanning electron microscopy (SEM), JEOL, Japan. TEM measurements were carried out using a carbon-coated copper grid as a photographic plate of the transmission electron microscope.

2.7. Thermogravimetric analysis

Thermogravimetric analysis (TGA) analysis using detector type Shimadzu TGA-50H with its component platinum cell, nitrogen atmosphere, and 20°C/min rate flowing.

2.8. Measurement of ammonia concentration

The concentration of ammonia was measured using a YSI photometer based on the indophenol method. Ammonia reacts with alkaline salicylate in the presence of chlorine to form a green-blue indophenol complex. Catalysts were incorporated to ensure complete and rapid color development. The reagents are provided in the form of two tablets for maximum convenience. The test was simply carried out by adding one of each tablet to a sample of the water. The intensity of the color produced in the test is proportional to the ammonia concentration and is measured using a YSI photometer.

2.9. Sampling of groundwater

Groundwater introduced to the study was collected from Al-Garnos and Shoulqam, Al-Minya, Egypt. Properties of groundwater samples before and after treatments are listed

in Table 1, which indicates a slightly decreasing of some properties such as turbidity, chloride contents, and total hardness and a considerable decrease in total dissolved salts.

3. Results and discussion

3.1. Synthesis and mechanisms aspects

The synthesis of poly(acrylamide-*co*-acrylate) was achieved as mentioned in the experimental section, but its hydrogel was performed in the presence of N,N′-methylenebisacrylamide as cross-linker. The quantity of cross-linker was chosen based on the yield of hydrogel to be 0.1 g (Fig. 1). TiO_2 nanoparticles were incorporated in the structure of acrylamide-*co*-acrylate hydrogel due to the presence of TiO_2 nanoparticles in the medium during the formation of hydrogel via both NH_x and/or OH groups (Fig. 2).

3.2. Characterization of obtained polymeric samples

Infrared spectroscopy of acrylamide-*co*-acrylate hydrogel in the presence and absence of TiO_2 nanoparticles is presented in Fig. 3. In addition, the absorption bands and their assignments are summarized in Table 2. Both Fig. 3 and Table 2 reveal that the main infrared bands of the acrylamide and acrylate and present. In addition, on the incorporation of TiO_2 in the structure of hydrogel, the bands indicate the interaction between Ti and both O and/or N-atoms are present.

XRD patterns of both hydrogel and its composite with TiO_2 are presented in Fig. 4 which indicates that hydrogel is amorphous but its composite seems to be nanocrystalline materials that clear from the peaks present in the broadband in the case of a composite.

SEM and TEM are presented in Fig. 5. SEM pictures show that the presence of TiO_2 in the structure of hydrogel leads to filling the pores of hydrogel and minimize the heterogeneous surface. The surface of the obtained composite is more compacted and smooth. In addition, TEM pictures reveal that the composite particle sizes (ranged from ~6.25 to 16.6 nm) are less than the hydrogel (ranged from ~18 to 50 nm). Also, there are significant variations in particle size in the case of hydrogel which becomes unclear in the case of a composite.

TGA of both hydrogel and composite are presented in Figs. 6 and 7. The temperature midpoints of thermal degradation are summarized in Table 3. From Figs. 6, 7 and Table 3, one can conclude that the water molecules absorbed by both hydrogel and composite are degraded at the end of 272°C. Also, the quantity of absorbed water in the case of a composite is higher which can be attributed to the interaction between TiO_2 and H_2O molecules. The higher residual quantity in the case of a composite is due to the presence of titanium in the carbonium residual part ~25%. All the above observations confirm the interaction between hydrogel chains and TiO_2.

Table 1
Groundwater properties

Parameter	Before	After
Turbidity, NTU	1.3	1.2
Chlorides, mg L^{-1}	140	130
Alkalinity, mg L^{-1}	320	320
Total dissolved salts, mg L^{-1}	710	650
Total hardness, mg L^{-1}	280	250
Ca hardness, mg L^{-1}	130	120
Mg hardness, mg L^{-1}	150	130

3.3. Removal of ammonia from groundwater using both fabricated hydrogel and it's composite

3.3.1. Effect of contact time

The effect of contact time on the adsorption capacity of the studied materials for ammonia was investigated using

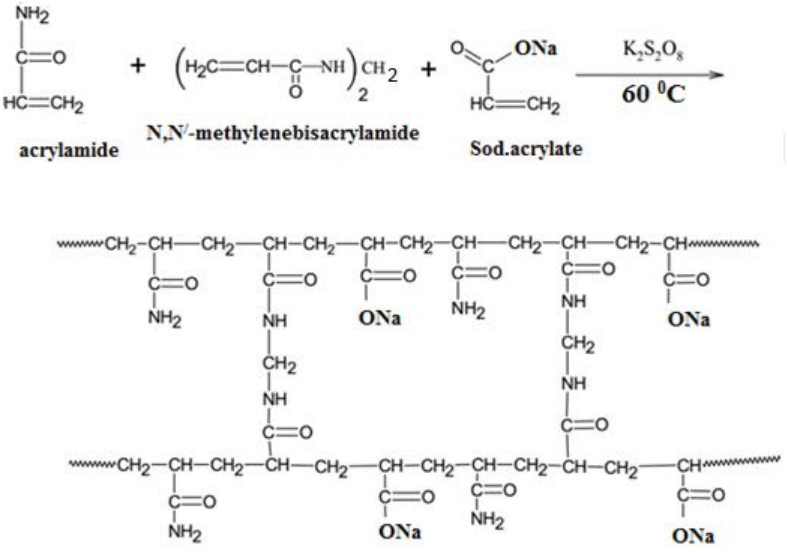

Fig. 1. Acrylamide/acrylate hydrogel.

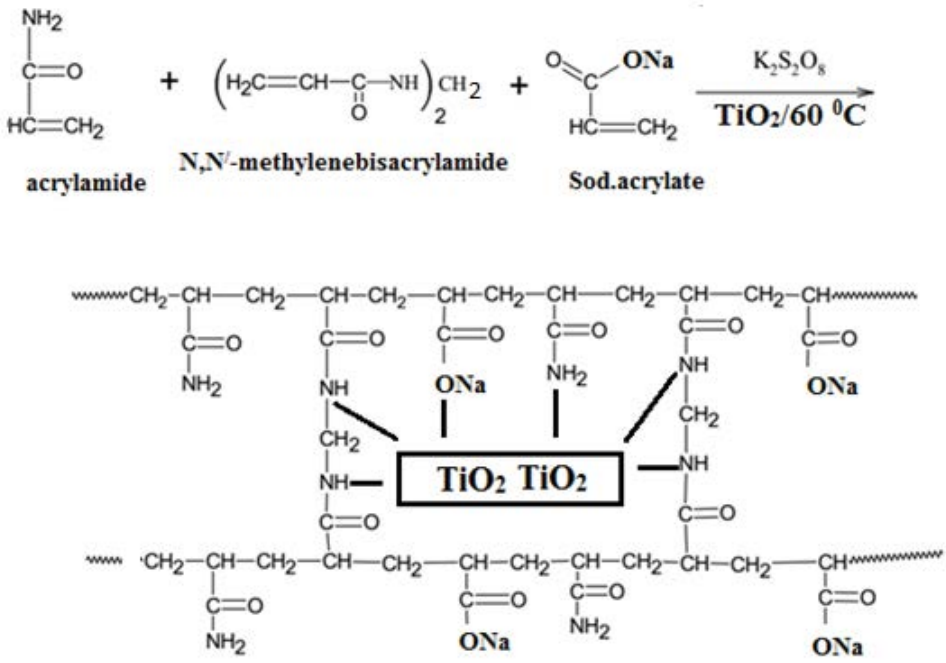

Fig. 2. Expected acrylamide/acrylate TiO_2 composite.

0.025–0.200 g of the hydrogel as adsorbents suspended in 100 mL of ammonia polluted solution (0.8 mg L^{-1}) for different time intervals time (10–90 min) as separated tests. After each time intervals, the residual ammonia concentrations were determined using YSI 9300 and 9500 photometers. All the experiments were performed at room temperature. Figs. 8 and 9 show that 0.2 g of the hydrogel is enough for complete removal of ammonia at 50 min, this quantity was reduced to 0.1 g which indicates the enhancing adsorption properties of the hydrogel by incorporation of TiO_2.

3.3.2. *Effect of adsorbents dose*

The effect of both hydrogel and their composite on the removal percentage of ammonia was investigated using different doses (0.01 to 0.25 g hydrogel and 0.01 to 0.1 g composite) at room temperature and contact time

Table 2
Infrared bands and their assignments

Wave number, cm^{-1}		Assignments [37]	References
Hydrogel	Hydrogel/TiO_2		
–	520^w	Ti bonded O	[37]
612^w	601^w	NH_2 torsion oscillation and/or Ti–N or Ti–O	
777^w	–	CH bending	
1,115^w	1,116^m	Stretching vibration of C–O and C–N stretching	[38]
1,176^w	1,181^w		[39]
1,334^w	1,325^m	CH_2 bending	[37]
1,409^m	1,405^s		
1,449^m	1,446^w		
–	1,567^s	C=O and/or adsorbed H_2O molecules and –COONa	[40]
1,656^s	1,667^s		
–	2,170^w	Overtone and combination bands	
2,376^w	2,372^w		
2,516^w	–	Aliphatic CH	[41]
2,859^w	–		
2,926^m	2,931^s		
3,422^b	3,426^b	Stretching vibration of OH and/or NH_2 free or bonded	[42]

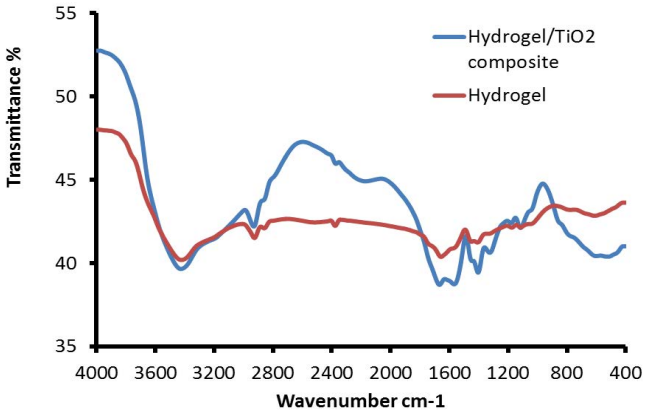

Fig. 3. Infrared of both poly(acrylate/acrylamide) hydrogel and their composite with TiO_2.

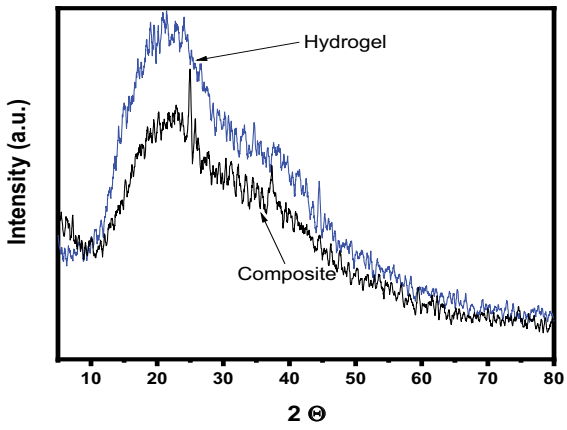

Fig. 4. X-ray diffraction patterns of both poly(acrylate/acrylamide) hydrogel and their composite with TiO_2.

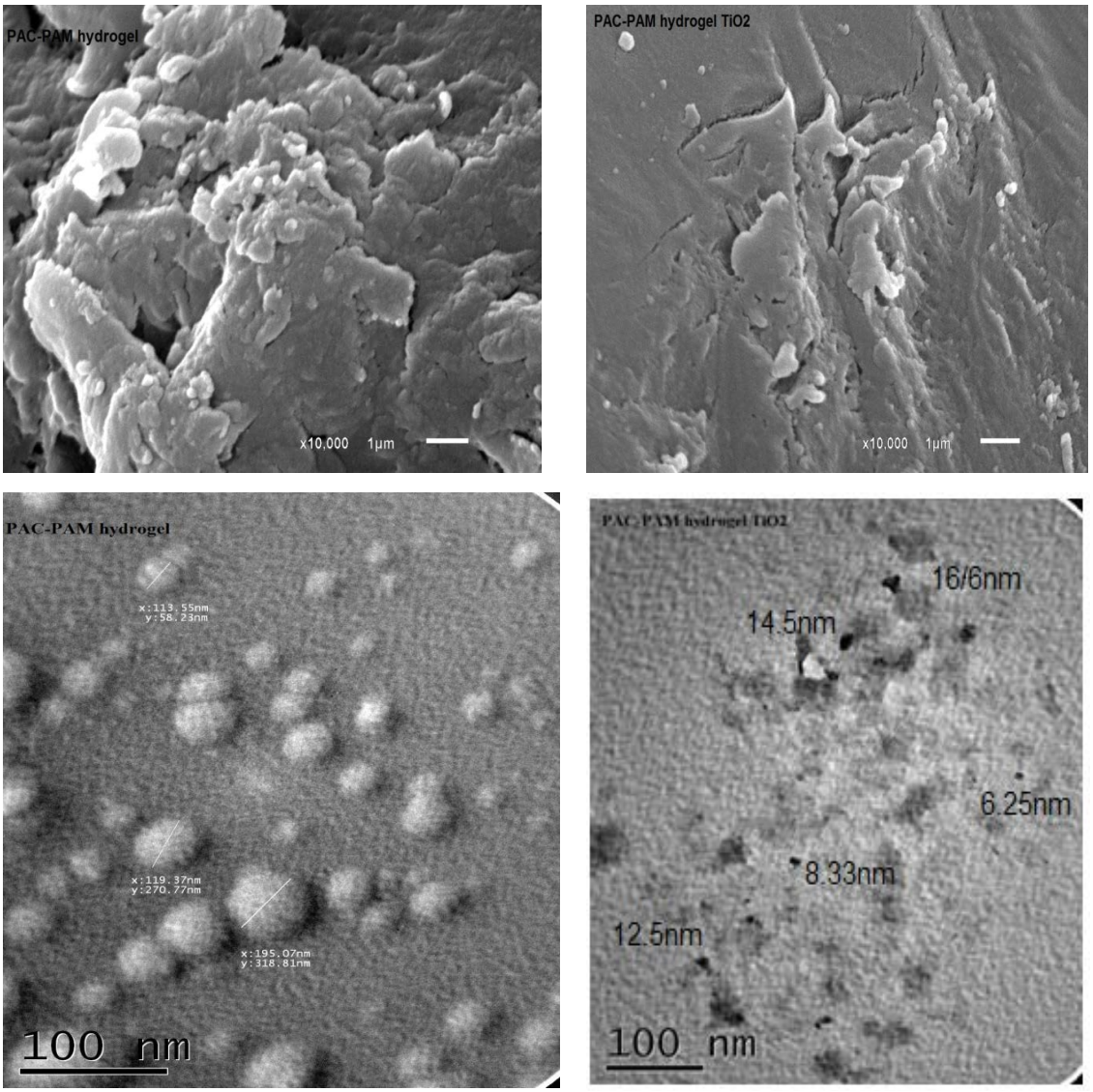

Fig. 5. Scanning and transmission electron microscopy for the fabricated hydrogel and their composite with TiO_2.

Table 3
TGA data of the fabricated samples

TGA parameters for polymeric samples				Comments
Hydrogel		Composite		
Midpoint, °C	Approx. wt. loss %	Midpoint, °C	Approx. wt. loss %	
73	4	69.5	10	Moisture losing
140	12	133.6	15	Bonded water loss
233	21	272	25	
335	38	318	32	Series of fragmentation of the polymer backbone depends on the bond strength between atoms
371	50	358	35	
403	52	–	–	
422	63	430	50	
466	72	–	–	
703	90	680	70	Complete degradation with the carbonic residue of about 10% in case of hydrogel but in case of composite the residue is about 25% which could be attributed to titanium corporation
–	–	722	75	

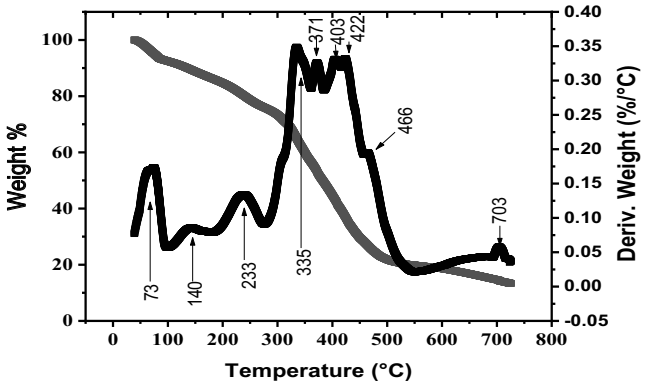

Fig. 6. TGA of the hydrogel.

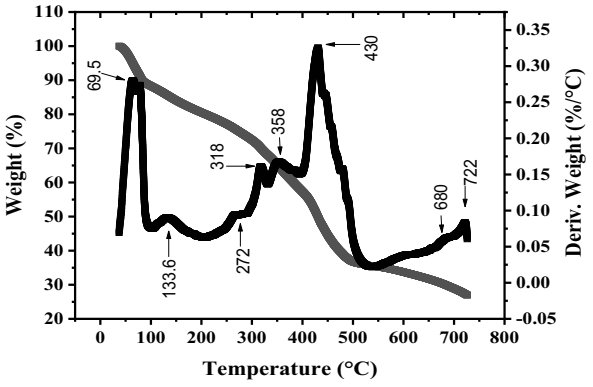

Fig. 7. TGA of hydrogel/TiO_2 composite.

50 min (Figs. 10–12). Data confirm the above results (100% removal by 0.2 g hydrogel and 0.1 g composite).

3.3.3. Effect of temperature and thermodynamics

The effect of temperature on the removal efficiency of 0.2 g hydrogel and 0.1 g composite on the removal of ammonia groundwater was studied for 50 min at different temperatures. The residual ammonia concentrations were determined using YSI 9300 and 9500 photometers after all temperatures and the removal % was plotted against temperature (Fig. 12). The obtained results reveal that the effect of temperature on the removal efficiency of both hydrogel and composite is considered poor and at higher temperatures have bad effects which could be attributed to the broken of physical adsorption of ammonia on the studied polymeric surface. In addition in the case of composite, the removal increase again at 323 K, we think that this removal is not due to adsorption but may be the result of the escaping of ammonia by the action of a composite. The thermodynamic parameters are deduced from the relations [8]:

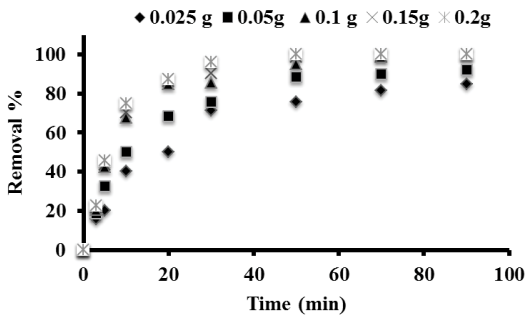

Fig. 8. Effect of contact time of removal efficiency of the hydrogel.

$$\Delta G^\circ = -RT\ln K_C \quad (1)$$

$$\Delta G^\circ = \Delta H^\circ - T\Delta S^\circ \quad (2)$$

$$\ln K_C = \frac{\Delta S^\circ}{R} - \frac{\Delta H^\circ}{RT} \quad (3)$$

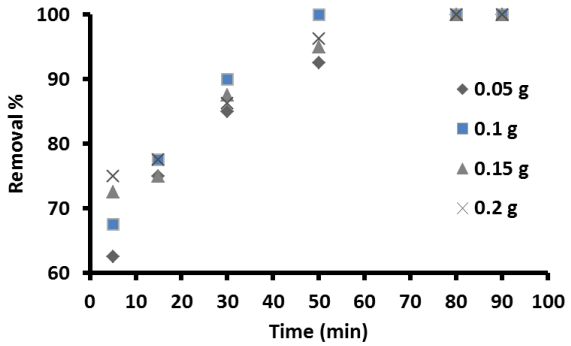

Fig. 9. Effect of contact time of removal efficiency of hydrogel/TiO_2 composite.

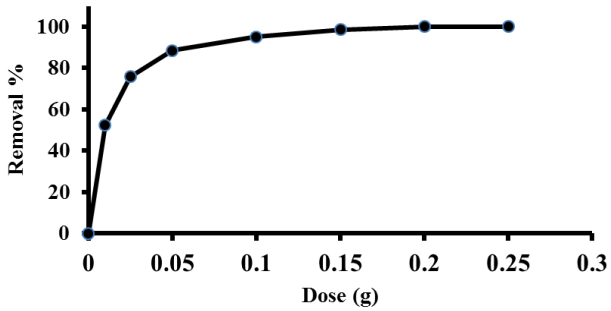

Fig. 10. Effect of doses of removal efficiency of the hydrogel.

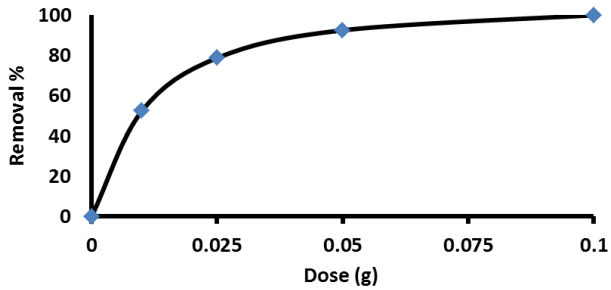

Fig. 11. Effect of doses of removal efficiency of hydrogel with TiO_2.

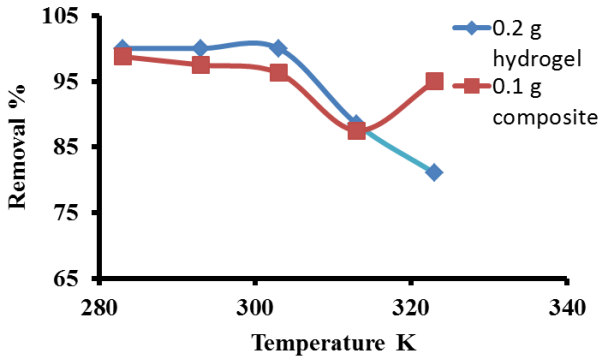

Fig. 12. Effect temperature on the removal efficiency of 0.2 g hydrogel and 0.1 g composite.

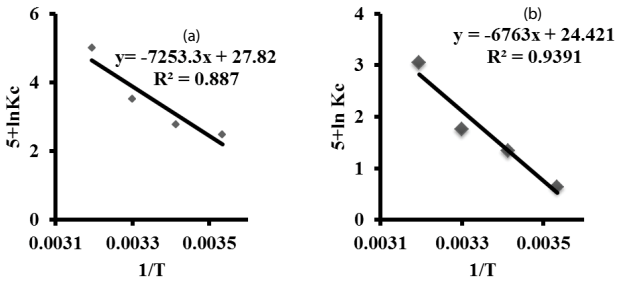

Fig. 13. Van't Hoff plot for the adsorption of ammonia on both (a) hydrogel and (B) composite.

where R is the general gas constant (8.314 J mol^{-1} K^{-1}), T is the absolute temperature in K_C is the Langmuir constant, ($\Delta H°$) is the standard enthalpy, and ($\Delta S°$) is the entropy of the adsorption process. The standard enthalpy $\Delta H°$ and the entropy of adsorption $\Delta S°$ could be estimated from the straight-line relationship between $\ln K_C$ vs. $1/T$ [43], (c.f. Fig. 13). The calculated data are summarized in Table 4. The obtained thermodynamic values reveal that the adsorption of ammonia on the surface of both hydrogel and their composite with TiO_2 is an exothermic and spontaneous process.

3.4. Adsorption isotherms

3.4.1. Langmuir isotherm

Langmuir adsorption linear form [44] is checked as a model for the adsorption of ammonia on polymeric surfaces in monolayer ordering fashion:

$$\frac{C_e}{q_e} = \frac{C_e}{Q_m} + \frac{1}{Q_{mb}} \tag{4}$$

Linear form (Fig. 14).

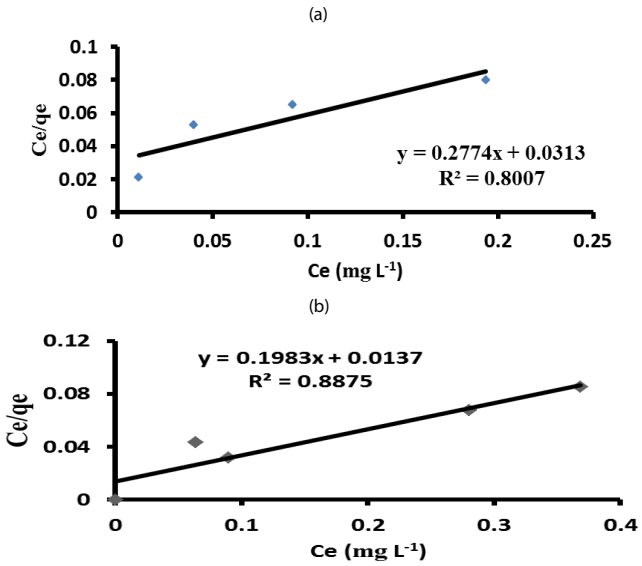

Fig. 14. Langmuir isotherm for (a) hydrogel and (b) composite.

Table 4
Thermodynamic parameters

Thermodynamic parameters		ΔG (kJ mol^{-1})	
		Hydrogel	Composite
Temperature (K)	283	–148.890	–144,331
	293	–151.203	–146,632
	303	–130.386	–125,928
	313	–132.699	–128,229
ΔH (kJ mol^{-1})		–60.3039	56.228
ΔS (J mol^{-1} K^{-1})		231.295	230.036

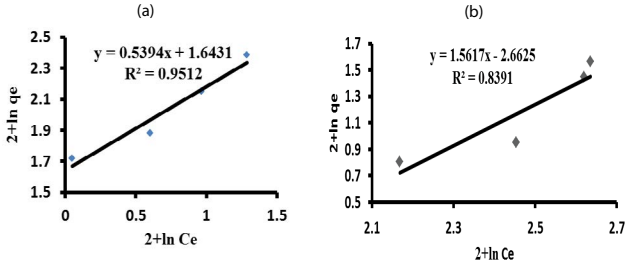

Fig. 15. Freundlich isotherm for (a) hydrogel and (b) composite.

3.4.2. Freundlich isotherm

Freundlich isotherm [45] is widely applied in the investigation of adsorption of different compounds. Here, the Freundlich model is used to analyze the adsorption results of ammonia on acrylamide/acrylate hydrogel and their TiO_2 composite, the equilibrium results are fitted with a logarithmic form of the Freundlich model.

$$\ln q_e = \ln K_f + \frac{1}{n}\ln C_e \tag{5}$$

The application of Temkin isotherm was also studied for adsorptions of ammonia on both hydrogel and their composite. Temkin model accepts that the energy of adsorption molecules decreases linearly with the surface coverage due to adsorbent/adsorbate interactions. The linear form of Temkin isotherm equation [46] was:

$$q_e = B_T \ln K_T + B_T \ln C_e \tag{6}$$

where q_e is the amount of adsorbed ammonia by the investigated polymeric sample at equilibrium (mg g^{-1}), K_f and n are dimensionless Freundlich constants related to the adsorption capacity and intensity, respectively; Q_m is the monolayer adsorption capacity (mg g^{-1}), b is a constant related to the adsorption equilibrium constant, C_e is ammonia concentration at equilibrium (mg L^{-1}).
where $B_T = RT/b$ is constant related to the heat of sorption (J mol^{-1}), and R is the ideal gas constant (8.314 J mol^{-1}), T is the absolute temperature (K), b is Temkin isotherm constant, and K_T is the Temkin isotherm equilibrium binding constant (L g^{-1}). The plots of C_e/q_e vs. C_e, $\ln q_e$ vs. $\ln C_e$ and q_e vs. $\ln C_e$ are shown in Figs. 14–16 and linear relationships are observed. All isothermic data are summarized in Table 5. The data show that hydrogel is followed by the Freundlich isotherm model but the composite is followed by Temkin isotherm.

3.4.3. Temkin isotherms

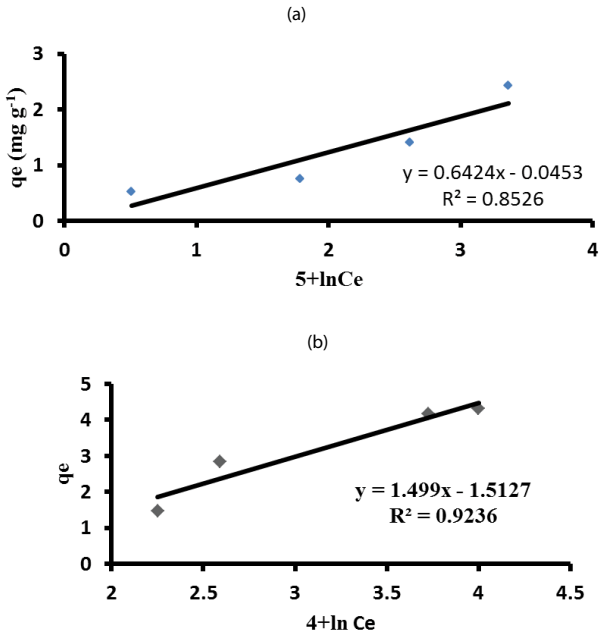

Fig. 16. Temkin isotherm for (a) hydrogel and (b) composite.

Table 5
Isothermic parameters for the adsorption of ammonia on hydrogel and their composite

Model	Isothermic parameters	Parameter values	
		Hydrogel	Composite
Langmuir	Q_m (mg g^{-1})	3.6	5.04
	b	8.86	14.48
	R^2	0.8007	0.8875
Freundlich	n	1.85	0.640
	K_f (mg g^{-1})	44	459
	R^2	0.9512	0.8391
Temkin	B_T (J mol^{-1})	0.6424	1.499
	K_T (L g^{-1})	0.955	0.22
	R^2	0.8526	0.9236

3.5. Adsorption kinetics

Two kinetic models were utilized to investigate the mechanism of adsorption of ammonia ions on the synthetic hydrogel and their composite from groundwater. The used models are the pseudo-first-order kinetic model [47].

$$\ln\left(q_e - q_t\right) = \ln q_e - k_1 t \tag{7}$$

Lagergren pseudo-second-order kinetic model [48]:

$$\frac{t}{q_t} = \frac{1}{k_2 q_0^2} + \frac{t}{q_e} \quad (8)$$

where q_t is the amount of adsorbed ions at time t (mg g^{-1}) and k_1 and k_2 are the rate constant of first and second-order adsorption (g mg^{-1} min^{-1}). Parameters of both first and second-order models were calculated from the slope and intercept of the linear plotting of $\ln(q_e - q_t)$ vs. t and (t/q_t) vs. t (Figs. 17 and 18). The obtained data are given in Table 6.

From the R^2 values, it is clear that the suitable model is the Lagergren pseudo-second-order kinetic model, which explains the chemical adsorption type which occurs through sharing between the used adsorbent materials and the dissolved ions beside the physical one [49]. The experimental adsorption capacity q_e (mg g^{-1}) was found to be 0.8 mg g^{-1} in both cases of hydrogel and its composite. The calculated one is 0.85 mg g^{-1} for both investigated samples which indicate the efficiency of present samples in ammonia removal at 30°C.

Table 6
Kinetic models data

Model	Parameter	Parameter value	
		Hydrogel	Composite
Pseudo-first-order	k_1 (min^{-1})	0.0642	0.0543
	q_e (mg g^{-1})	12.2	177.5
	R^2	0.8801	0.8675
Pseudo-second-order	k_2 (min^{-1})	0.21	0.28
	q_e (mg g^{-1})	0.80	0.80
	R^2	0.9999	0.994

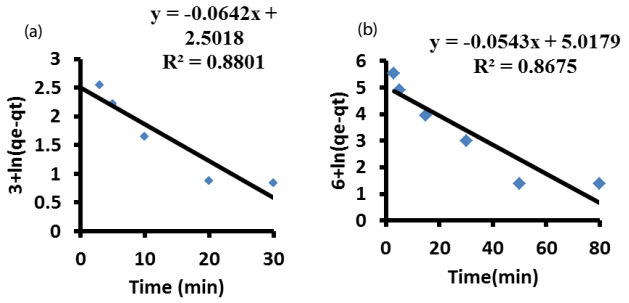

Fig. 17. Pseudo-first and second-order kinetic model for both hydrogel (a) and composite (b).

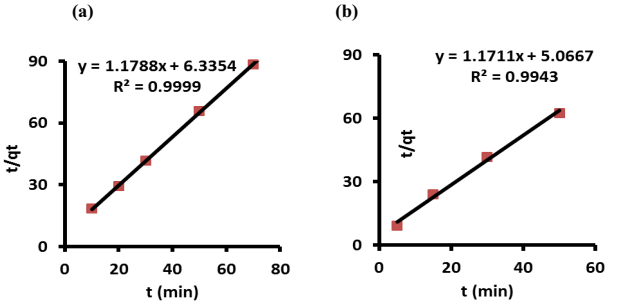

Fig. 18. Pseudo-second-order kinetic model for both hydrogel (a) and composite (b).

4. Conclusion

It is necessarily known that water is the lifeblood and that some countries, even where there are rivers, need to use groundwater. The researchers' mission is to check this water to make it suitable for use. Researches have shown the presence of ammonia in groundwater. Therefore, researchers must remove ammonia from water at the lowest cost and in fast time. The polymeric compounds used in this research are easy to prepare and inexpensive. And the obtained results showed its efficiency to remove ammonia from the water.

Acknowledgment

The authors thank the Faculty of Science, Beni-Suef University, Egypt, for continued financial supporting.

References

[1] P.L. Younger, Groundwater in the environment: an introduction, Oxford, Blackwell Publisher, Malden, MA, 2007 p. 318.
[2] H.H. Dieter, R. Möller. Ammonia, K. Aurand et al., Eds., Die trinkwasserverordnung, einführung und erläuterungen. The Drinking-Water Regulations, Introduction and Explanations, Erich-Schmidt Verlag, Berlin, 1991, pp. 362–368.
[3] P. Hadi, E. Soheil, H. Mohammad, H. Amirhossein, Comparison of zeolite (clinoptilolite) and activated carbon, in ammonia removal during transport of live rainbow trout fry (*Oncorhynchus mykiss*), J. Nat. Environ., Iran. J. Nat. Resour., 66 (2013) 255–260.
[4] A.G. Tekerlekopoulou, D.V. Vayenas, Ammonia, iron and manganese removal from potable water using trickling filters, Desalination, 210 (2007) 225–235.
[5] J. Lindenbaum, Identification of Sources of Ammonium in Groundwater Using Stable Nitrogen and Boron Isotopes in Dam Du, Hanoi, Master Thesis, Lund University, Lund, Sweden, 2012.
[6] M. Shaban, M.R. Abukhadra, M.G. Shahien, A.A.P. Khan, Upgraded modified forms of bituminous coal for the removal of safranin-T dye from aqueous solution, J. Environ. Sci. Pollut. Res., 24 (2017) 18135–18151.
[7] WHO, Guidelines for Drinking-Water Quality, 3rd ed., Incorporating the First and Second Addenda Volume 1, Recommendations, World Health Organization, Geneva, Switzerland, 2008.
[8] A. Alshameri, A. Ibrahim, A.M. Assabri, X.R. Lei, H.Q. Wang, C.J. Yan, The investigation into the ammonium removal performance of Yemeni natural zeolite: modification, ion exchange mechanism, and thermodynamics, Powder Technol., 258 (2014) 20–31.
[9] N. Taneva, Removal of ammonium and phosphates from aqueous solutions by activated and modified Bulgarian clinoptilolite, J. Chem. Eng. Mater. Sci., 3 (2012) 79–85.
[10] W.H. Xiong, J. Peng, Development and characterization of ferrihydrite-modified diatomite as a phosphorus adsorbent, Water Res., 42 (2008) 4869–4877.
[11] D.V. Vayenas, S. Pavlou, G. Lyberatos, Development of a dynamic model describing nitritification and nitratification in trickling filters, Water Res., 31 (1997) 1135–1147.
[12] A. Wilczak, J.G. Jacangelo, J.P. Marcinko, L.H. Odell, G.J. Kirmeyer, Occurrence of nitrification in chloraminated distribution systems, J. Am. Water Works Assn., 88 (1996) 74–85.

[13] H.X. Huo, H. Lin, Y.B. Dong, H. Cheng, H. Wang, L.X. Cao, Ammonia-nitrogen and phosphates sorption from simulated reclaimed waters by modified clinoptilolite, J. Hazard. Mater., 229 (2012) 292–297.
[14] H.M. Abd El-Salam, R.A. Mohamed, A. Shokry, Preparation and characterization of novel and selective polyacrylamide-graft-poly(2-methoxyaniline) adsorbent for lead removal, Polym. Bull., 75 (2018) 3189–3210.
[15] H.M. Abd El-Salam, E.H.M. Kamal, M.S. Ibrahim, Synthesis and characterization of chitosan-grafted-poly(2-hydroxyaniline) microstructures for water decontamination, J. Polym. Environ., 25 (2017) 973–982.
[16] T. Hatva, H. Seppanen, A. Vuorinen, L. Carlson, Removal of iron and manganese from groundwater by re-infiltration and slow sand filtration, Aqua Fennica, 15 (1985) 211.
[17] T. Hatva, Treatment of Groundwater with Slow Sand Filtration, Proceedings International Groundwater Microbiology. Problems and Biological Treatment, Kuopio, Finland, 4–6 August 1987.
[18] P. Mouchet, From conventional to biological removal of iron and manganese in France, J. Am. Water Works Assn., 84 (1992) 158.
[19] H.A. Abd El-Rehim, E.A. Hegazy, A. El-Hag Ali, Selective removal of some heavy metal ions from sing treated polyethylene-*g*-styrene/maleic anhydride membranes, React. Funct. Polym., 43 (2000) 105–116.
[20] M.A. Shaker, Adsorption of Co(II), Ni(II) and Cu(II) ions onto chitosan-modified poly(methacrylate) nanoparticles: dynamics, equilibrium and thermodynamics studies, J. Taiwan Inst. Chem. Eng., 57 (2015) 111–112.
[21] N. Thanh Ha, D.D. Khanh, H.T. Ngan, T.H. Quang, P.L. Huong, D.T. Hung, Nitrification of high levels of ammonia in groundwater using fixed-bed biofiltration technique, Vietnam J. Chem., 57 (2019) 75–79.
[22] S. Tabassum, A combined treatment method of novel mass bio system and ion exchange for the removal of ammonia nitrogen from micro-polluted water bodies, Chem. Eng. J., 378 (2019) 122217, https://doi.org/10.1016/j.cej.2019.122217.
[23] A.K. Maharjan, T. Kamei, I.M. Amatya, K. Mori, F. Kazama, T. Toyama, Ammonium-nitrogen (NH_4^+–N) removal from groundwater by a dropping nitrification reactor: characterization of NH_4^+–N transformation and bacterial community in the reactor, Water, 12 (2020) 599, https://doi.org/10.3390/w12020599.
[24] N.A.H. Mohamad Zaidi, L.B.L. Lim, A. Usman, Enhancing adsorption of Pb(II) from aqueous solution by NaOH and EDTA modified *Artocarpus odoratissimus* leaves, J. Environ. Chem. Eng., 6 (2018) 7172–7184.
[25] N. Priyantha, L.B.L. Lim, N.H. Mohd Mansor, A.B. Liyandeniya, Irreversible sorption of Pb(II) from aqueous solution on breadfruit peel to mitigate environmental pollution problems, Water Sci. Technol., 80 (2019) 2241–2249.
[26] L.B.L. Lim, N. Priyantha, Y.C. Lu, N.A.H. Mohamad Zaidi, Adsorption of heavy metal lead using *Citrus grandis* (Pomelo) leaves as low-cost adsorbent, Desal. Water Treat., 166 (2019) 44–52.
[27] H. Abdulrazzaq, H. Jol, A. Husni, R. Abu-Bakr, Characterization and stabilization of biochars obtained from empty fruit bunch, wood, and rice husk, J. Bioresour., 9 (2014) 98–2888.23
[28] S. Balci, Y. Dinçel, Ammonium ion adsorption with sepiolite: use of transient uptake method, J. Chem. Eng. Process., 41 (2002) 79–85.
[29] M.S. Çelik, B. Özdemir, M. Turan, I. Koyuncu, G. Atesok, H.Z. Sarikaya, Removal of ammonia by natural clay minerals using fixed and fluidized bed column reactors, J. Water Supply, 1 (2001) 81–98.
[30] A. Demir, A. Günay, E. Debik, Ammonium removal from aqueous solution by ion-exchange using packed bed natural zeolite, J. Water SA, 8 (2002) 329–335.
[31] C.C. Hollister, J.J. Bisogni, J. Lehmann, Ammonium, nitrate, and phosphate sorption to and solute leaching from biochars prepared from corn stover (*Zea mays* L.) and oak wood (Quercus ssp.), J. Environ. Qual., 42 (2013) 137–144.
[32] D. Tang, Z. Zheng, Z. Guo, Study on ammonia-nitrogen adsorption from low concentration waste water by modified zeolite and its desorption, Chin. J. Environ. Eng., 5 (2011) 293–296.
[33] M. Tian, Z. Zeng, Z. Jiang, Progress of preparation and applications of bamboo charcoal, J. Mater. Rev., 29 (2015) 143–146.
[34] S.R. Paudel, B.R. Kansakar, Dissolved ammonia adsorption in water using over burnt brick, Energy Res. J., 1 (2010) 1–5.
[35] M. Shaban, M.R. Abukhadra, F.M. Nasief, H.M. Abd El-Salam, Removal of ammonia from aqueous solutions, groundwater, and wastewater using mechanically activated clinoptilolite and synthetic zeolite-A: kinetic and equilibrium studies, Water Air Soil Pollut., 228 (2017) 450.
[36] Q.J. Li, J.W. Zhang, B.B. Liu, M. Li, R. Liu, X.L. Li, H.L. Ma, S.D. Yu, L. Wang, Y.G. Zou, Z.P. Li, B. Zou, T. Cui, G.T. Zou, Synthesis of high-density nanocavities inside TiO_2–B nanoribbons and their enhanced electrochemical lithium storage properties, Inorg. Chem., 47 (2008) 9870–9873.
[37] R.M. Silverstein, F.X. Webster, D.J. Kiemle, D.L. Bryce, Spectrometric Identification of Organic Compounds, Wiley, New York, 1974.
[38] S.N. Monteiro, F.M. Margem, R.L. Loiola, F.S. de Assis, M.P. Oliveira, Characterization of banana fibers functional groups by infrared spectroscopy, Mater. Sci. Forum, 775–776 (2014) 250–254.
[39] M.C. Paiva, I. Ammar, A.R. Campos, R.B. Cheikh, A.M. Cunha, Alfa fibres: mechanical, morphological and interfacial characterization, Compos. Sci. Technol., 67 (2007) 1132–1138.
[40] K.R. Reddy, K.-P. Lee, A.I. Gopalan, Novel electrically conductive and ferromagnetic composites of poly(aniline-*co*-aminonaphthalene sulfonic acid) with iron oxide nanoparticles: synthesis and characterization, J. Appl. Polym. Sci., 106 (2007) 1181–1191.
[41] B. Dan-asabe, A.S. Yaro, D.S. Yawas, S.Y. Aku, I.A. Samotu, U. Abubakar, D.O. Obada, Mechanical, spectroscopic and micro-structural characterization of banana particulate reinforced PVC composite as piping material, Tribol. Ind., 38 (2016) 255–267.
[42] C. Rojas, M. Cea, A. Iriarte, G. Valdés, R. Navia, J.P. Cárdenas-R, Thermal insulation materials based on agricultural residual wheat straw and corn husk biomass, for application in sustainable buildings, Sustainable Mater. Technol., 20 (2019) e00102, https://doi.org/10.1016/j.susmat.2019.e00102.
[43] X.J. Peng, Z.K. Luan, H.M. Zhang, Montmorillonite–Cu(II)/Fe(III) oxides magnetic material as adsorbent for removal of humic acid and its thermal regeneration, Chemosphere, 63 (2006) 300–306.
[44] C. Namasivayam, R.T. Yamuna, Adsorption of direct red 12 B by biogas residual slurry: equilibrium and rate processes, Environ. Pollut., 89 (1995) 1–7.
[45] H. Freundlich, W.J. Helle, J. Am. Chem. Soc., 61 (1939) 2–28.
[46] M.J. Temkin, V. Pyzhev, Kinetics of ammonia synthesis on promoted iron catalysts, Acta Physiochimica URSS, 12 (1940) 217–222.
[47] S.Y. Lagergren, Zur Theorie der sogenannten Adsorption gelöster Stoffe, Kungliga Svenska Vetenskapsakademiens. Handlingar, 25 (1898) 1–39.
[48] Y.S. Ho, G. McKay, Pseudo-second-order model for sorption processes, Process Biochem., 34 (1999) 451–465.
[49] K.S. Hui, C.Y.H. Chao, S.C. Kot, Removal of mixed heavy metal ions in wastewater by zeolite 4A and residual products from recycled coal fly ash, J. Hazard. Mater., 127 (2005) 89–101.